BEAM OBSERVATIONS IN THE P.L.A.*

K. Batchelor
Rutherford Laboratory

This report discusses some measurements recently made on the Rutherford P.L.A., using a precise time-of-flight technique. The time-of-flight system is described in the report: "An Accurate Determination of the P.L.A. Beam Energy by a Time-of-Flight Method", NIRL/R/9, (1961), by C.J. Batty and D.J. Warner. The time-of-flight system is also discussed in "P.L.A. Progress Report No. 1", (1961) and the measurements will be mentioned in "P.L.A. Progress Report No. 2", to be published shortly.

The experimental arrangement for these measurements is shown in Fig. 1. The proton beam passes through a series of quadrupole doublets and two scattering chambers. Flip-in scintillators, viewed by television, are used to monitor the beam. Each scattering chamber contains a .0002" aluminum foil, the distance between the foils defining the flight path. The scintillation counters detect only elastically scattered protons, and are maintained at an identical distance from the foil in both scattering locations, so that only the flight time between the two foils is measured.

The electronics associated with one of these scintillation counters is shown in Fig. 2. An rf beam deflector is used between the preinjector and the linac, providing burst of protons separated by 88.89 nsec. The rf deflection voltage also provides, after suitable pulse forming, timing pulses separated by 88.89 nsec, accurately phased with respect to the proton bursts. These pulses provide the "stop" pulses for the time analyzer. The "slow"

*Report of work done by A.P. Banford, K. Batchelor, C.J. Batty, A. Carne, J.M. Dickson, D.J. Warner.

pulse from the 13th dynode of the photomultiplier 56AVP is used to gate out pulses corresponding to inelastic events. A time to amplitude converter is used, which is described in A.E.R.E. R2903, by F.H. Wells and A.K. Barlow.

The flight path is chosen to give flight times of 7 x 89 nsec, 4 x 89 nsec, and 3 x 89 nsec, corresponding to proton energies of 10, 30, and 50 Mev, respectively. The actual flight path is 25.75 meters.

The scattering foil in the "Y" section shown in Fig. 1 is flipped, to avoid unnecessary background at the second counter. The second counter at the first scattering location is used to provide reference spectra, to prevent that slight drifts affect the results when the other counter is moved between the first and second scatterer.

It was noticed during the first measurements that the existing rf power monitor did not give an adequate indication of the level in the cavity. To carry out measurements to an accuracy commensurate with the time-of-flight system, the acceptance phase was measured for each tank, and used as a criterion of rf level in the tank.

For the measurements of acceptance phase, it is necessary to have a small phase spread in the input beam. The rf deflector provides bunches of protons separated by 88.89 nsec, with an inherent width of about 2.25 nsec. In addition, axial fields at the entrance and exit of the deflector provide some bunching, which might reduce this width to about 1.5 nsec. Radial acceptance of the linac may reduce this figure further. This corresponds to a width of 70^{o} to 90^{o} in phase, which, of course, is not an ideal spread to use, but does suffice to give some idea of the acceptance phase for the first tank.

The results of the acceptance phase measurements on tank 1, are shown in Fig. 3, for three different rf levels.

Assuming that the tank voltage, taken as the square root of a reflectometer forward power reading, is proportional to sec ϕ_s and the acceptance width, the full width at half-height of the curves of Fig. 3, is equal to $K\phi_s$, where ϕ_s is the stable phase angle, then the experimental results yield K= 2.75. This is in fairly good agreement with the theoretical value of 3 .

Plotting now beam current as a function of beam energy for various tank rf power levels, curves as shown in Fig. 4 are obtained. This figure refers to the output of tank 1. The actual design energy for tank 1 is calculated to be 9.87 Mev. The experimental results agree quite well with this.

The output beam current from tank 2, is shown in Fig. 5, for different tank 1 power levels. There is quite a pronounced variation in the tank 2 output energy, even though the input energy remains fairly constant as indicated in Fig. 4. There are two reasons for this behavior. First, for tank 2 the ϕ_s value is 30^o, which happens to correspond to an odd number of quarter wave phase oscillations, thus giving a bigger effect. Secondly, the input design energy for tank 2 is 9.91 Mev, while the actual output energy of tank 1 is 9.87 Mev, a discrepancy of about 40 kev. This difference will superimpose on the normal phase oscillations and will act to enhance the observed effect.

Another interesting effect can be seen from Fig. 5. Above a level of about 450 kw for tank 1, the tank 2 output current decreases very noticeably, although the corresponding decrease in tank 1 is not large. This is not explainable in terms of the acceptance of the second tank, if one considers just the phase motion. It is possible that this is some radial motion effect, but at the present, it is unexplained.

The rf system is shown schematically in Fig. 6. In all of the measurements quoted here, the phase in degree has been taken directly from the line stretcher length. This might be incorrect, due to a mismatch. However, this section has been very carefully matched, and it is felt that errors arising from this should be quite small.

The acceptance phase for tank 2 is shown in Fig. 7. Here, although the input phase spread to tank 1 may be of the order of 70° to 80°, phase damping in the first tank reduces this spread to something of the order of 30° entering the second tank.

A comparison of the stable phase angle, as calculated from the measured acceptance phase, and its theoretical values, based on the tank voltage being proportional to sec ϕ_s, is given in Fig. 8.

A theoretical curve of the number of quarter wave phase oscillations as a function of the rf level in tank 2 is shown in Fig. 9.

The variation of beam energy with input phase for different rf levels in tank 2 is given in Figs. 10, 11, 12, 13 and 14. Conversion factors for phase shifter settings are indicated along the graphs. The amplitudes of the curves are proportional to the beam current. Each curve refers to a fixed phase shifter setting indicated along the ordinate axis. The tank 2 rf power level of 895 kw corresponds to an integral number of half wave phase oscillations, which explains the observed small energy change with input phase variation for this particular rf level.

The results of these 5 diagrams are summarized in Fig.15 and compared to the corresponding theoretical curves. Although the agreement is not precise, the theoretical and experimental curves clearly have the same character.

Theoretical curves for the variation of output energy with input phase, for various input energies are shown in Fig. 16. All of these curves have the same general shape, which justifies, to some extent, the comparison of theoretical and experimental curves shown in Fig. 15 for somewhat different synchronous phase angles, e.g. a 33.5^{o} experimental value as compared with a 35^{o} theoretical value.

Acceptance phase measurements were done for tank 3, with substantially the same results as for the second tank. These curves showed narrower peaks, however, as might be expected since the phase spread of the bunches has been reduced in going through the second tank. These measurements indicate that ϕ_s in the third cavity is about 20^{o}.

The design energy for tank 3 is 49.74 Mev, which has not yet been reached. It is felt that when the power level in the third tank is increased to give $\phi_s = 30^{o}$, full design energy will be attained.

The effect of a symmetrical field tilt on the output energy of tank 3 is shown in Fig. 17. The numbers for input tilt refer to positions of the tilt tuners.

A symmetrical tilt indicated in Fig. 17 at value 70 yields the highest energy measured so far, but this is still below design energy.

The output energy versus input phase for tank 3, with that tilt which gives the highest energy, is shown in Fig. 18.

Accurate energy measurements have been made with the machine under normal operating conditions. The results are summarized below:

	Measured Energy	Design Energy	Stable Phase Angle
Tank 1	9.870 ± 0.005 Mev	9.880 Mev	$30^{o} \pm 3^{o}$
Tank 2	30.45 ± 0.03 Mev	30.46 Mev	$30^{o} \pm 3^{o}$
Tank 3	49.50 ± 0.05 Mev	49.74 Mev	$20^{o} \pm 3^{o}$

Actually, tank 1 was designed to give 9.915 Mev, but it was found that the tank dimensions were not quite correct, and the theoretical energy was recomputed to 9.880 Mev. The $\pm$ 3° phase errors are quite enough to account for any variations from the design energy in the first two tanks. Tank 3 has not yet achieved a stable phase angle of 30°, for which it was designed.

From the results presented in the foregoing, it is possible to determine the effect of rf level changes on the output beam of each section. These results are:

Tank 1

at 10 Mev: 0.5 kev/kw, or about 0.05% energy change for 1% change in tank voltage.

at 30 Mev: 10 kev/kw, or about 0.3% energy change for 1% change in tank voltage.

Tank 2

at 30 Mev: 2 kev/kw, i.e. 0.13% energy change for a 1% change in tank voltage; a phase change between tank 1 and 2 of 1° gives a 25 kev energy change, i.e. 0.1% energy change /°ϕ.

Tank 3

The rf level has not been measured here, but a phase change of 1° between tank 2 and tank 3 gives an energy change of 30 kev, i.e. 0.1% energy change/°ϕ.

This is for ϕ_s = 20°, which is not the design value.

As a result of these measurements, some changes are being made in the P.L.A. New monitors are being installed, with which it is hoped to reproduce the tank fields to 0.1%. It is planned to maintain this precision with a servo system.

A detector bridge has been linked between the first and second cavity, to determine the effects of any possible changes in phase between these two

tanks. The accuracy of measurement is better than 0.1^{o}. The results indicate:

1) There is a warm up period of 10 to 15 minutes after a trip-out of about 5 minutes duration , during which time, the inter-tank phase has a maximum error of 4^{o}, reducing to zero at the end of this period.

2) There is a random variation of $\pm 1^{o}$ over a period of 15 minutes. This is thought to be due to variations in drive level to the grounded grid triodes. This supposition has been checked by actually varying this drive. An auto-level control on the drive appears to have cured this problem. High voltage variations on the grounded grid triodes do not have such a large effect.

3) A long term drift on the order of 5^{o} over a 24 hour period has been noted. This could be a temperature effect, but is not explained yet.

4) There are short term variations of $\pm .25^{o}$ over periods of 15 to 30 seconds. This effect is being investigated further, and could be due to servo hunting in the auto-tuning.

Discussion

R.P. Featherstone (Minnesota): Referring to the acceptance phase measurements for tank 1, is it significant that the best beam current was observed at the lowest rf level?

K. Batchelor (Rutherford): It is significant here. We normally set up the machine in fact to give maximum beam current from tank 1. If one plots beam current versus rf level, one finds a lower threshold of about 380 kw, an optimum level of around 415 kw and a falling-off above this.

L.C. Teng (ANL): How do you explain the fall-off?

K. Batchelor (Rutherford): This is due to grid focusing in the first tank.

H.B. Knowles (Yale): Do you have any curves of beam output at various rf levels versus preinjector voltage?

K. Batchelor (Rutherford): We do not at the moment. This is planned for the future. There are so many parameters possible for this measurement that we have not been able to explore them all.

H.B. Knowles (Yale): Have you ever noticed an abrupt change in the beam output level under conditions of almost no change of external parameters?

K. Batchelor (Rutherford): We have not in the course of these measurements. Experimentalists have claimed to notice this effect at times. We have always been known to explain it off, I think, in terms of their equipment.

H.B. Knowles (Yale): The 32 Mev proton linac at Berkeley had sudden changes in energy during operation, usually following a spark, but sometimes it just happened; it was finally concluded that this was due to the effect known as "oil-canning". The tank liner would heat up and go either out or in. The directions were entirely random, and the magnitudes were too.

K. Batchelor (Rutherford): We had some "oil-canning" with some tuners during the early stages of the machine, but certainly not with the tank liner itself, which has a fair number of supporting ribs.

J.P. Blewett (BNL): The 0.1^{o} phase measurements between tank sections is made by setting a null on the measuring bridge and looking at the position of a line stretcher?

K. Batchelor (Rutherford): Yes.

ACCELERATOR PHYSICS

Mr. A.P. BANFORD, Mr. K. BATCHELOR, Mr. A. CARNE, Mr. J.M. DICKSON, Mr. D. J. WARNER.

THE APPARATUS IS USED TO DETERMINE THE OUTPUT ENERGY OF EACH SECTION OF THE P.L.A. UNDER VARIOUS OPERATING CONDITIONS. TIME-OF-FLIGHT METHOD IS USED TO INCREASE THE SPACING BETWEEN PROTON BURST FROM 5 NANO SECONDS TO 89 NANO SECONDS AND THE FLIGHT TIME BETWEEN TWO THIN ALUMINIUM SCATTERING FOILS SEPARATED BY 25·75 METRES IS MEASURED. THIS TIME IS MEASURED TO AN ACCURACY OF 0·1 NANO SECOND TO GIVE THE REQUIRED ACCURACY FOR THE ENERGY MEASUREMENT.
(N.B. 1 NANO SECOND = $\frac{1}{1,000,000,000}$ SECOND.)

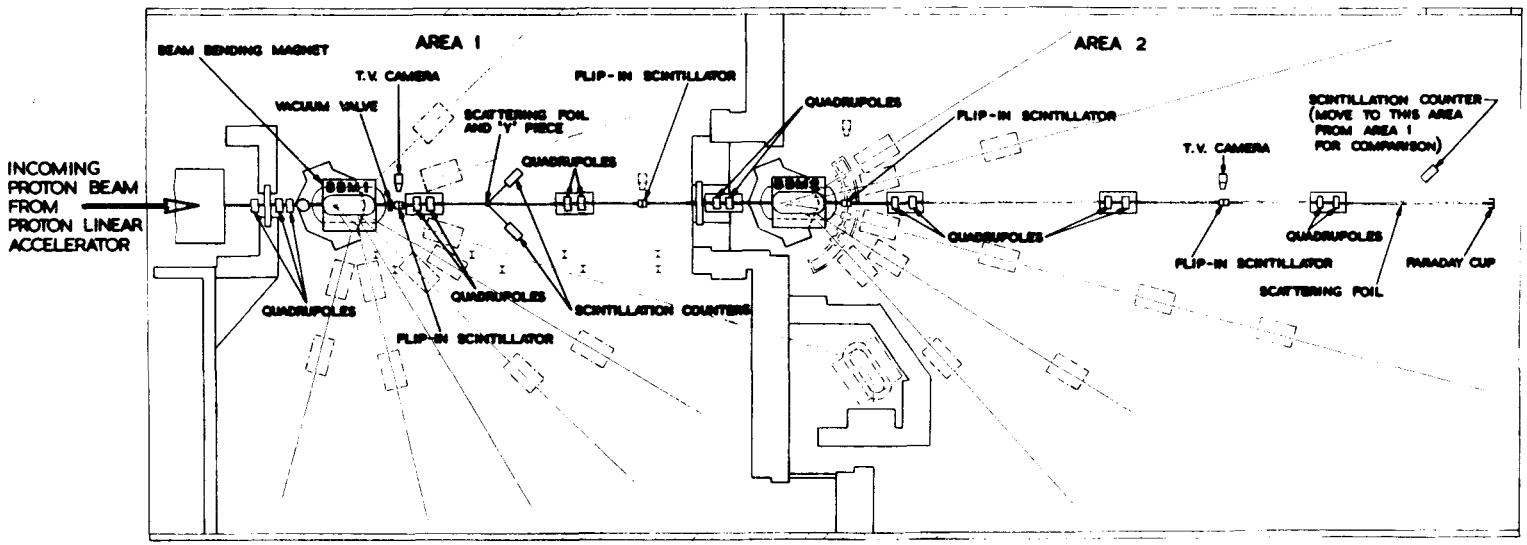

PLEASE NOTE: FOR EASE OF ACCESS - CERTAIN ITEMS OF EQUIPMENT HAVE BEEN REMOVED.

Fig. 1

Proceedings of the 1962 Conference on Linear Accelerators for High Energies, Upton, New York, USA

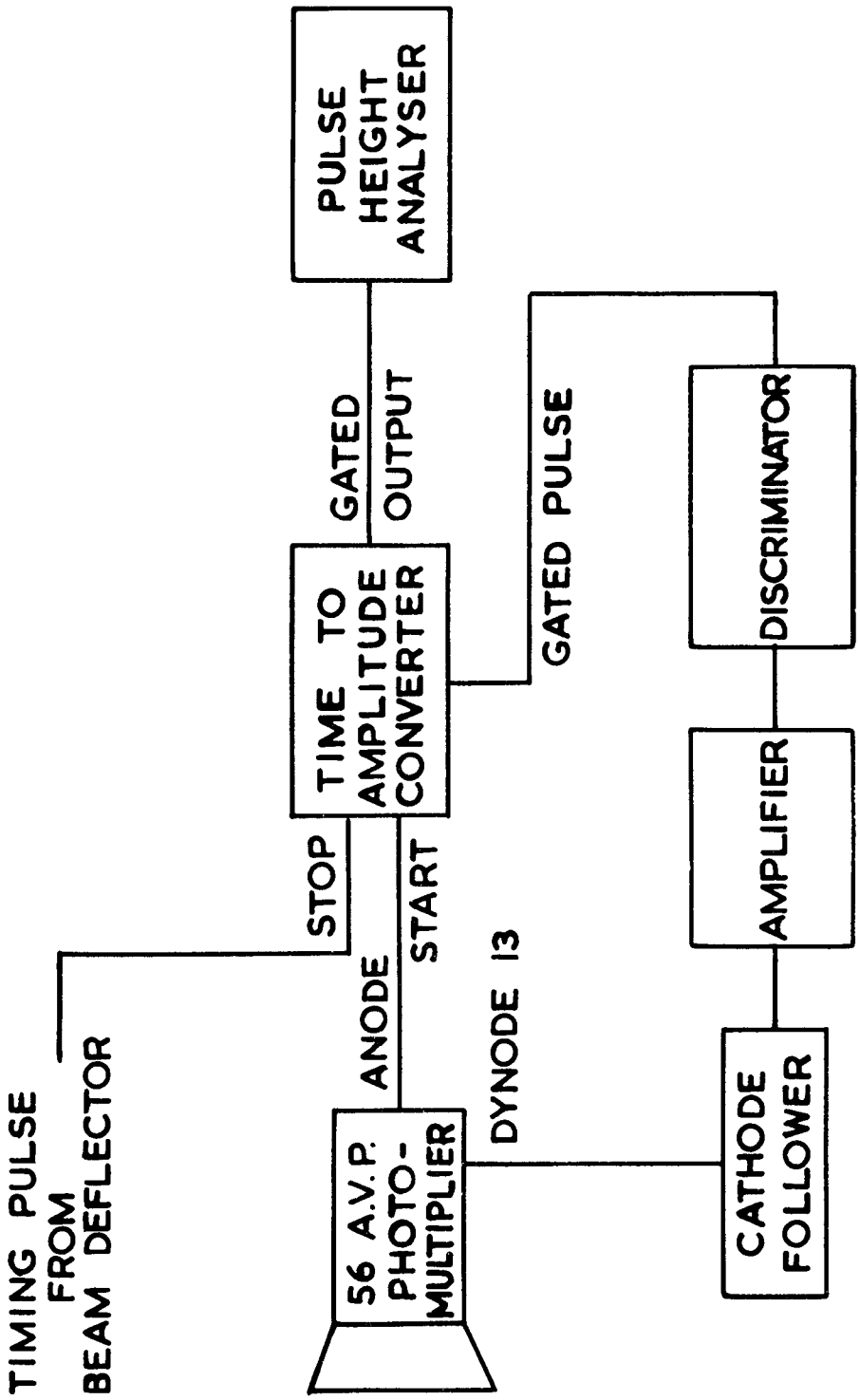

Fig. 2

BLOCK DIAGRAM OF ELECTRONICS

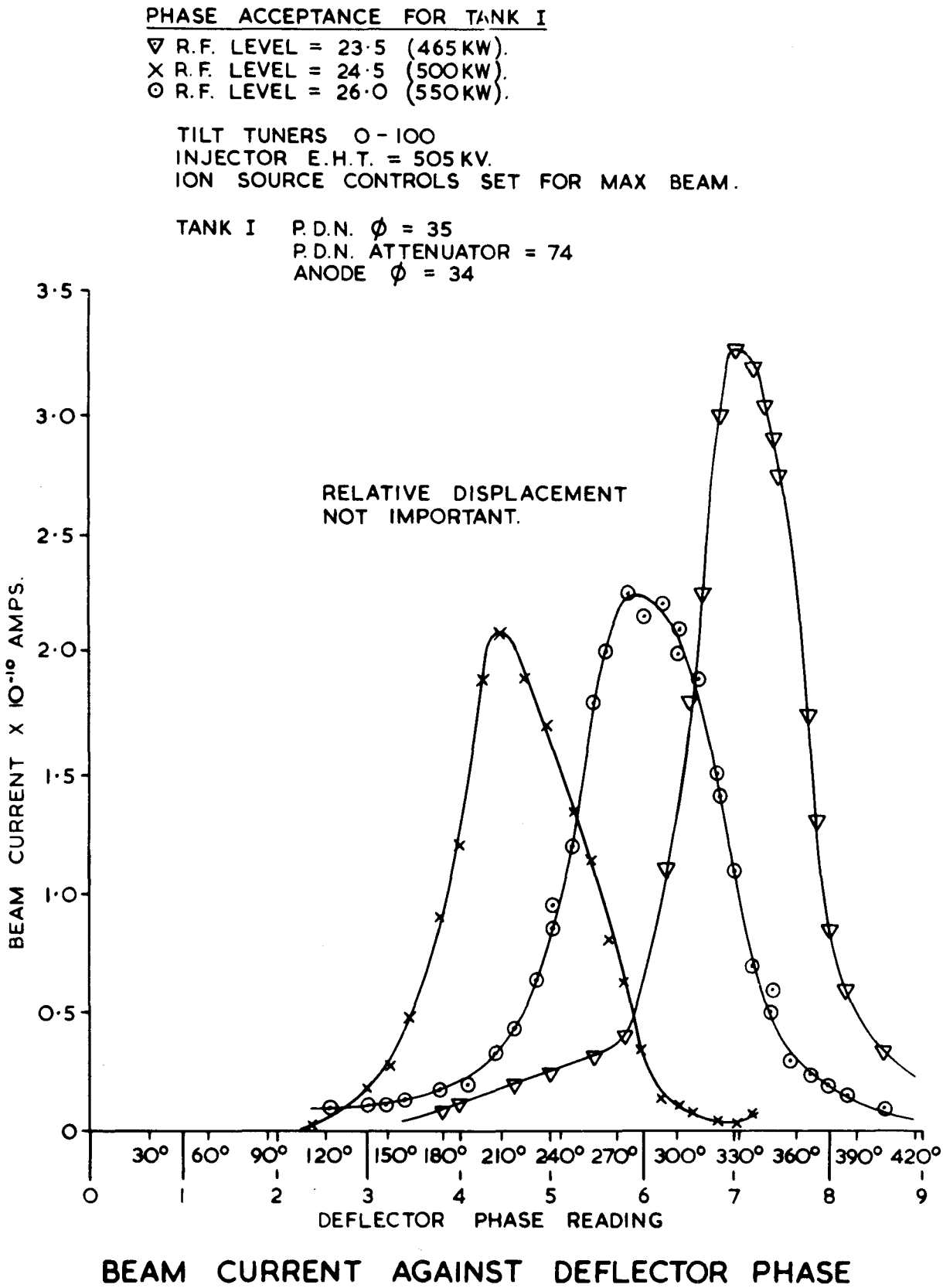

BEAM CURRENT AGAINST DEFLECTOR PHASE

Fig. 3

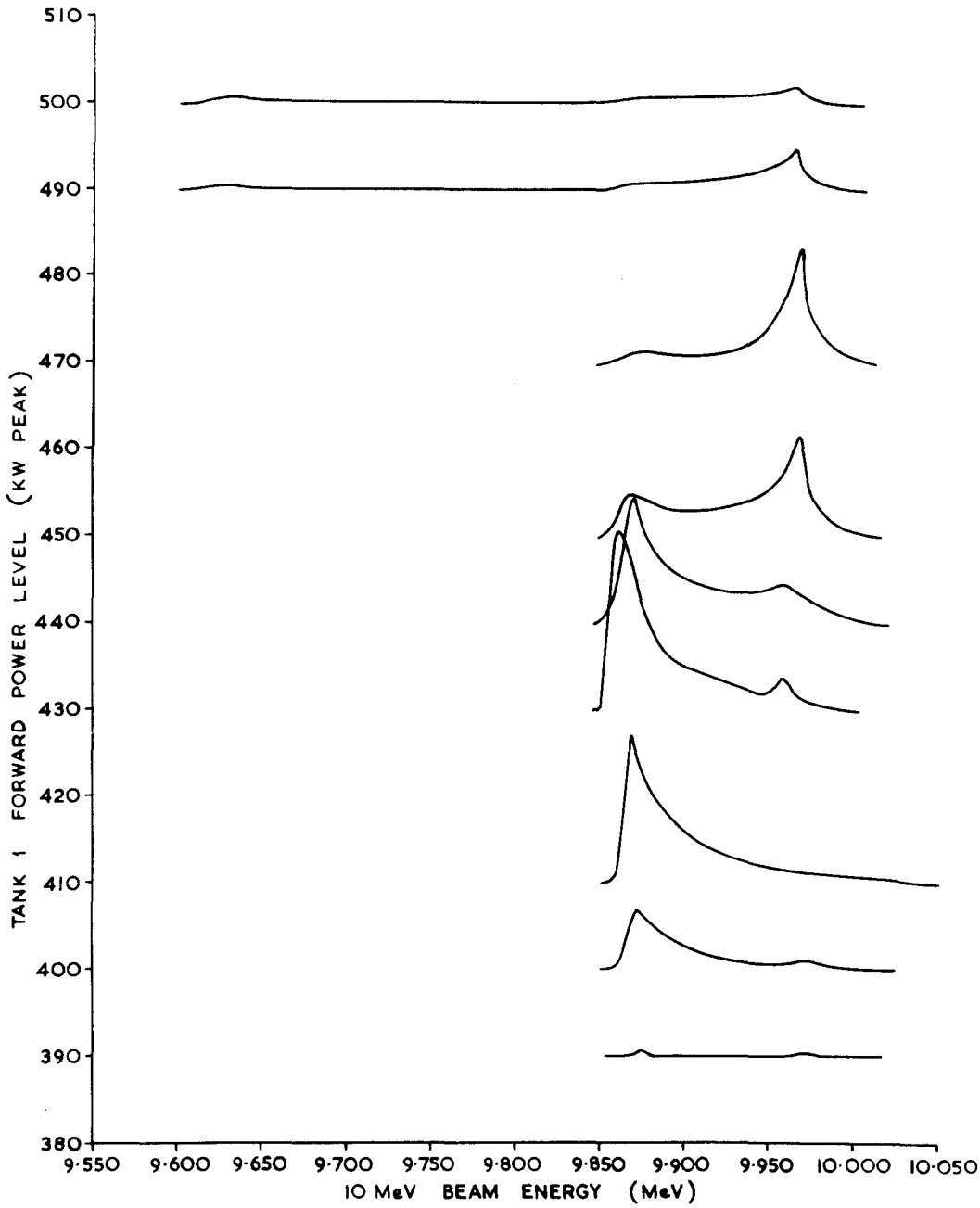

10 MeV ENERGY v R.F. LEVEL

Fig. 4

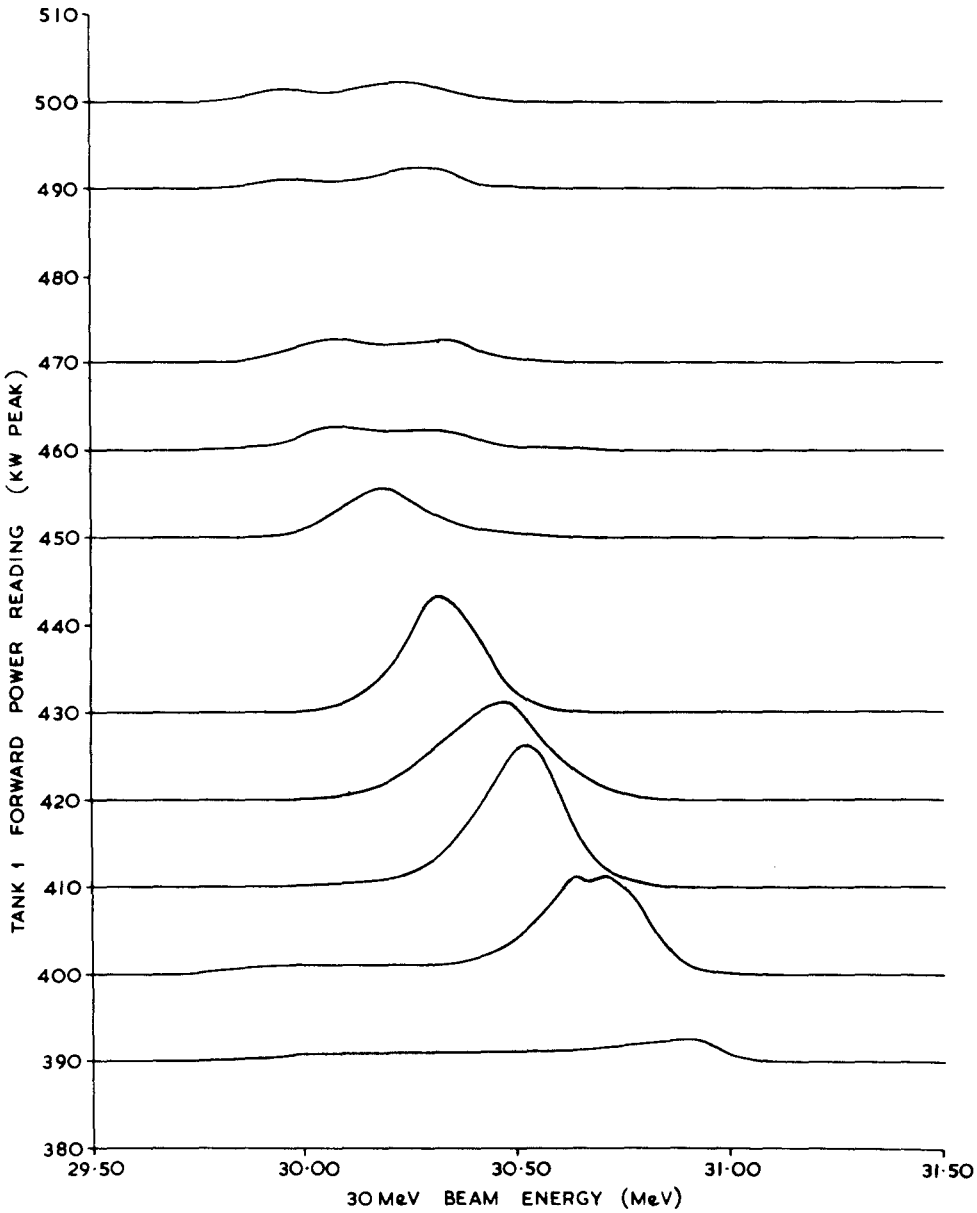

30 MeV BEAM ENERGY AND CURRENT AS A FUNCTION OF R.F. LEVEL IN TANK 1

Fig. 5

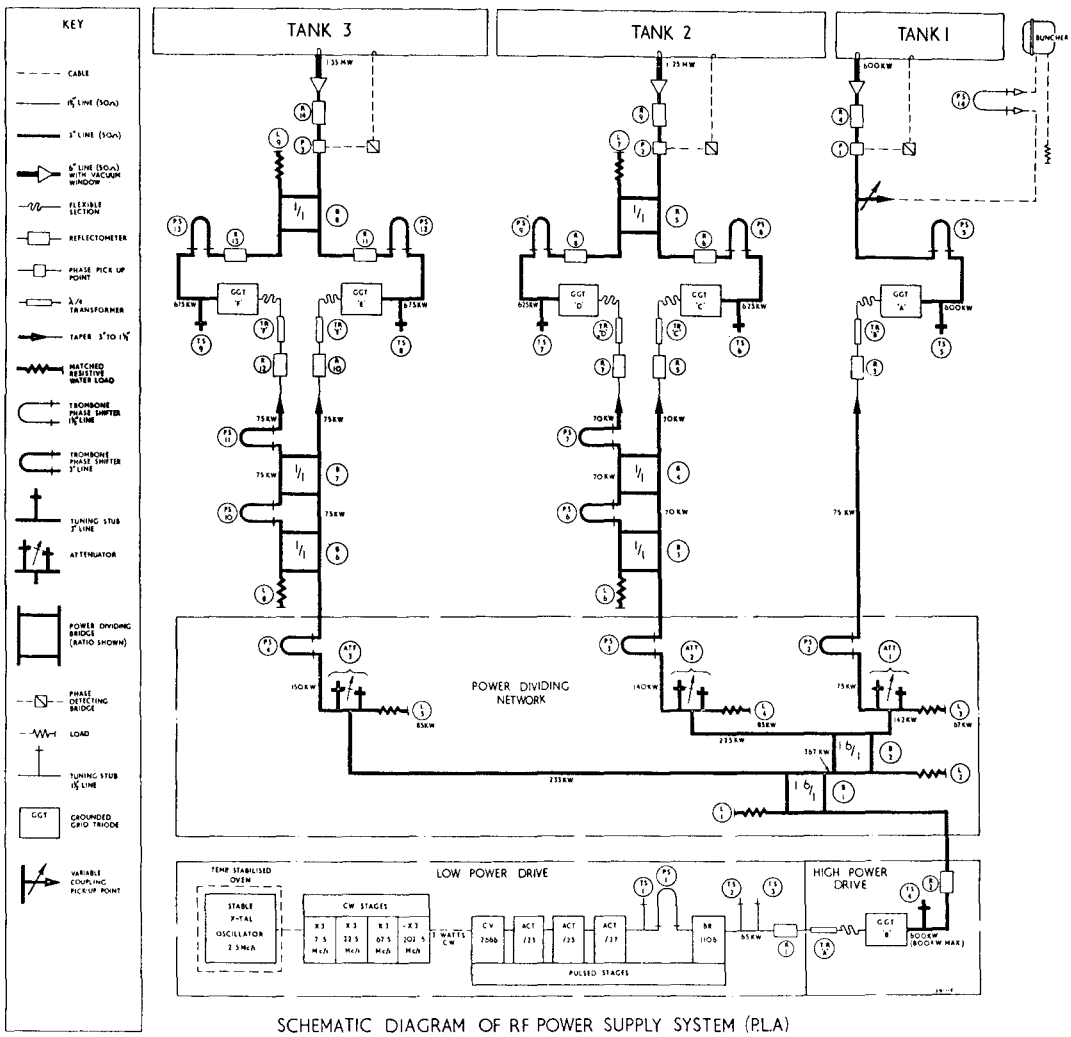

SCHEMATIC DIAGRAM OF RF POWER SUPPLY SYSTEM (P.L.A)

H.61/2013.a.

Fig. 6

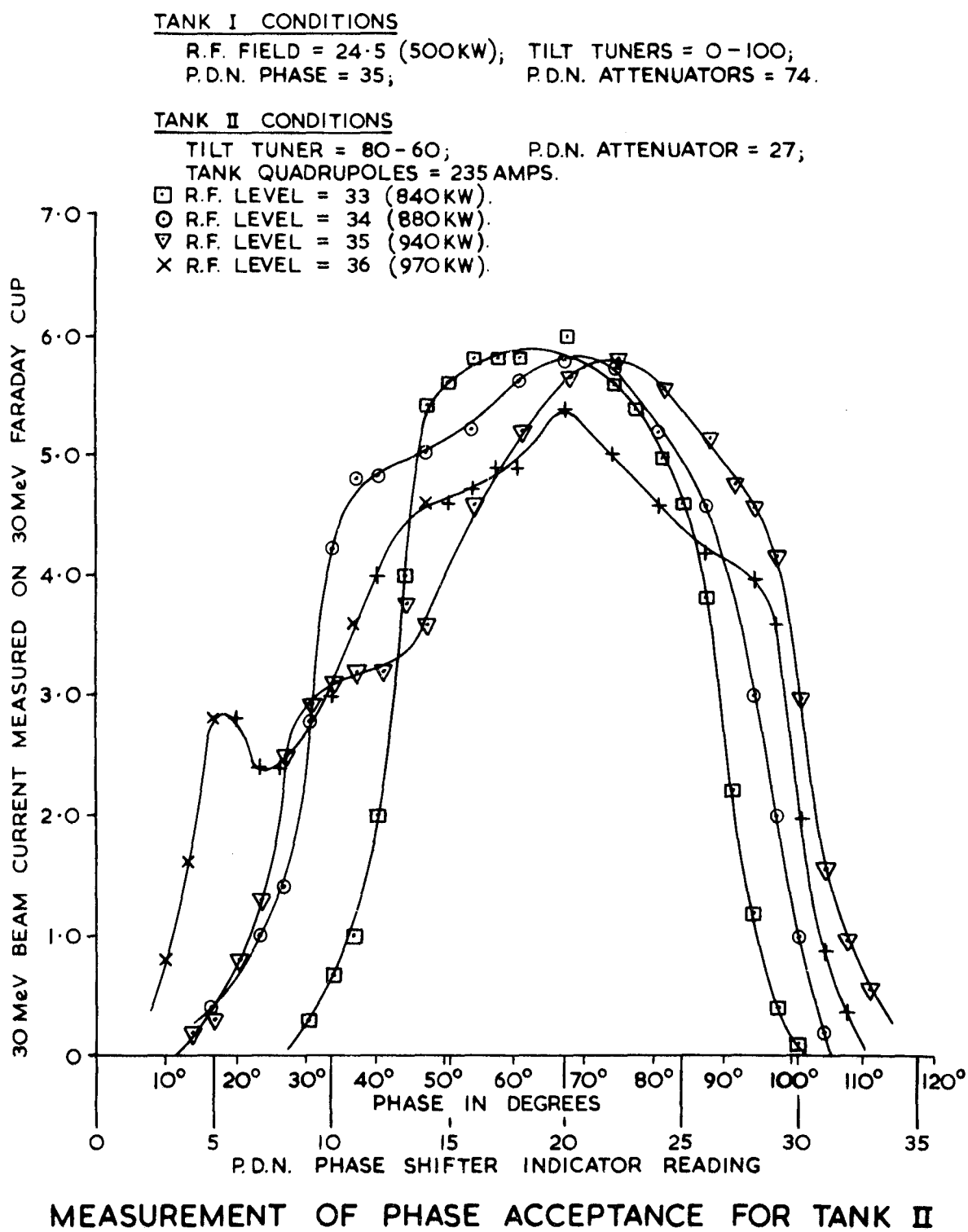
TANK I CONDITIONS
R.F. FIELD = 24·5 (500KW); TILT TUNERS = 0 – 100;
P.D.N. PHASE = 35; P.D.N. ATTENUATORS = 74.
TANK II CONDITIONS
TILT TUNER = 80 – 60; P.D.N. ATTENUATOR = 27;
TANK QUADRUPOLES = 235 AMPS.
R.F. LEVEL = 33 (840KW).
R.F. LEVEL = 34 (880KW).
R.F. LEVEL = 35 (940KW).
R.F. LEVEL = 36 (970KW).
30 MeV BEAM CURRENT MEASURED ON 30 MeV FARADAY CUP
7·0
6·0
5·0
4·0
3·0
2·0
1·0
0
10° 20° 30° 40° 50° 60° 70° 80° 90° 100° 110° 120°
PHASE IN DEGREES
0 5 10 15 20 25 30 35
P.D.N. PHASE SHIFTER INDICATOR READING
MEASUREMENT OF PHASE ACCEPTANCE FOR TANK II

Fig. 7

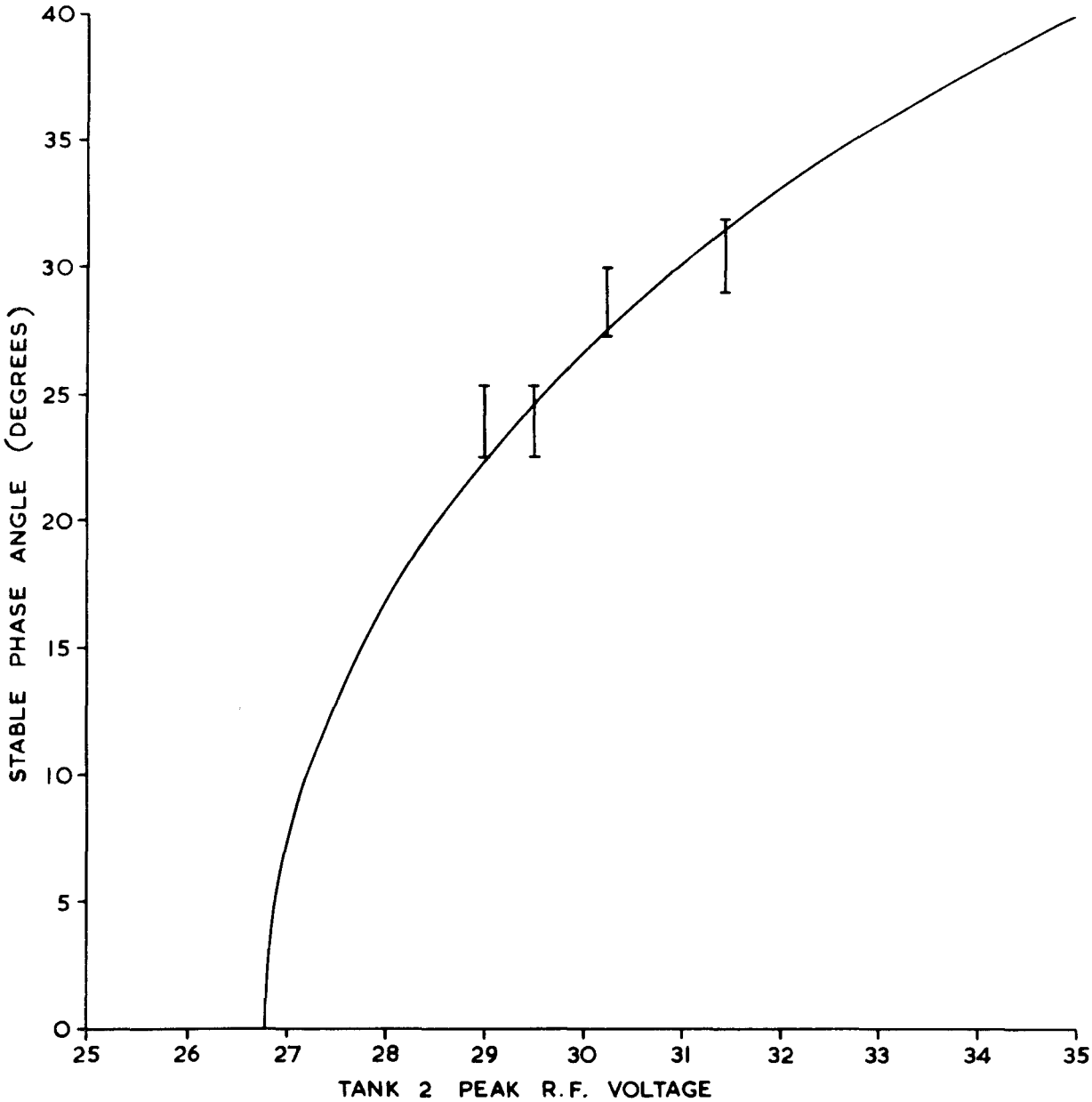

STABLE PHASE ANGLE v TANK 2 R.F. VOLTAGE

Fig. 8

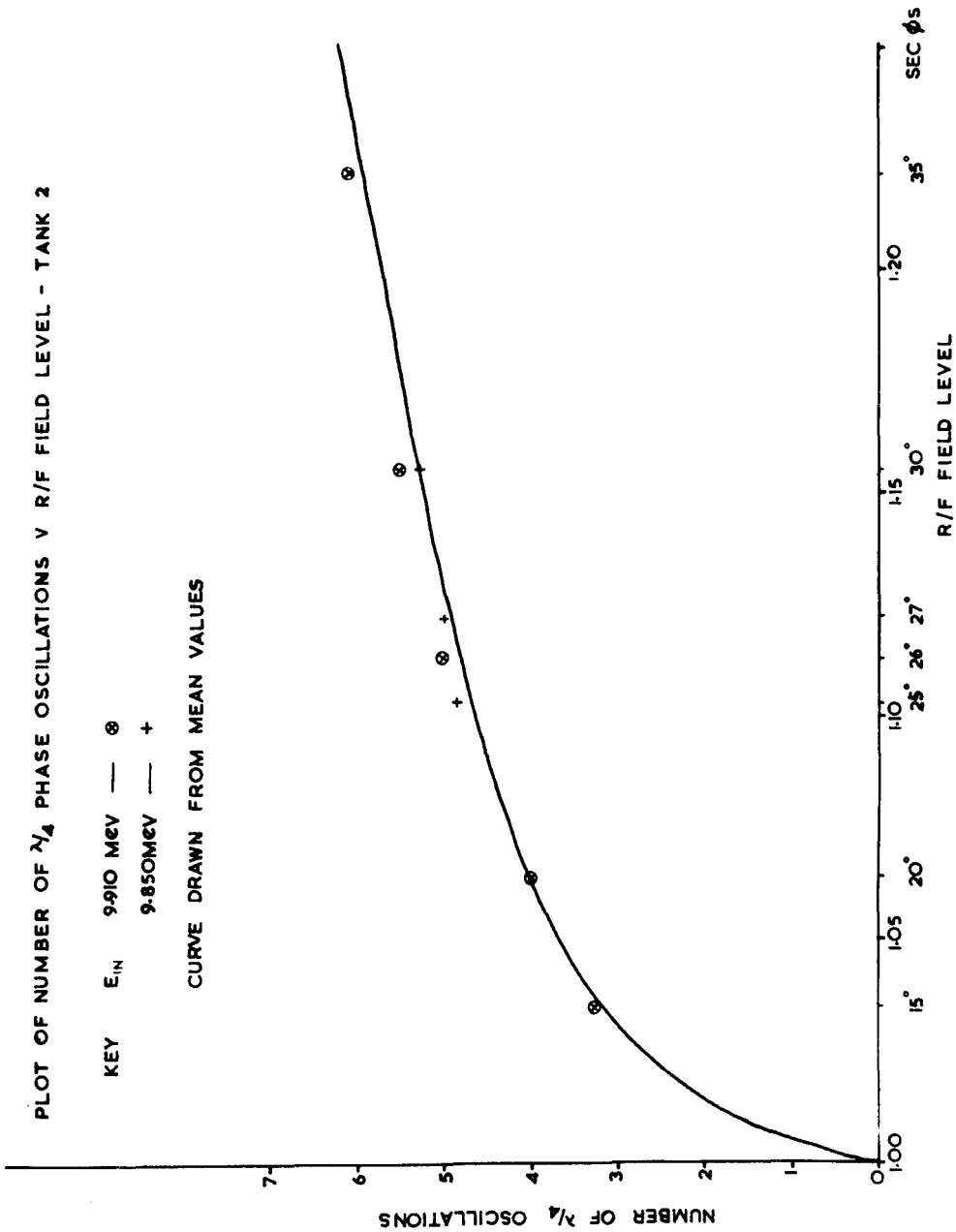
PLOT OF NUMBER OF λ/4 PHASE OSCILLATIONS V R/F FIELD LEVEL - TANK 2
KEY E_IN 9.910 MEV — ⊗
9.850MEV — +
CURVE DRAWN FROM MEAN VALUES
NUMBER OF λ/4 OSCILLATIONS
0
1
2
3
4
5
6
7
1.00
15°
1.05
20°
1.10
25°
26°
27°
1.15
30°
1.20
35°
SEC ϕs
R/F FIELD LEVEL

Fig. 9

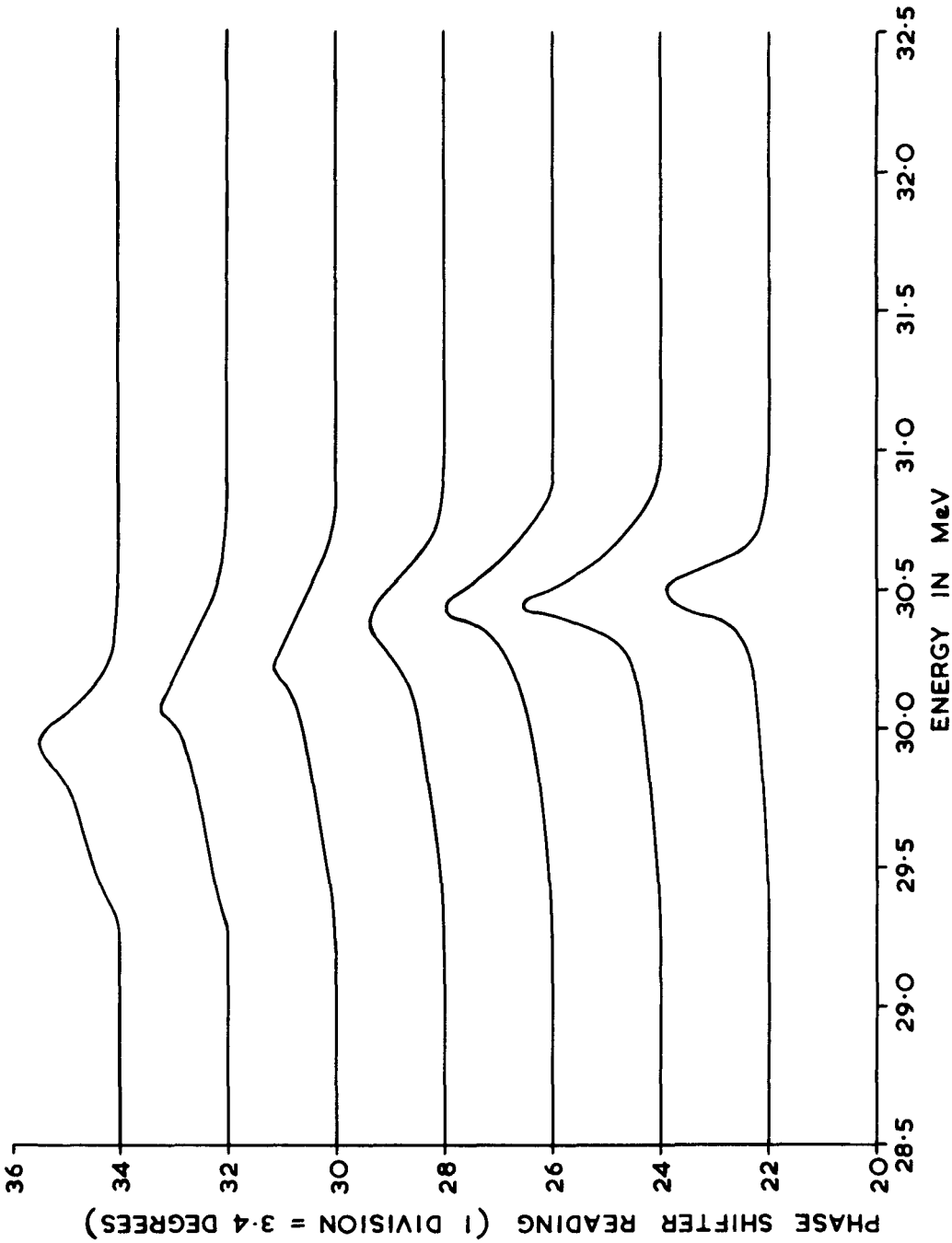
30 MeV ENERGY v INPUT PHASE
TANK 2 R.F. LEVEL = 33·0 (850 KW)
ENERGY IN MeV
28·5
29·0
29·5
30·0
30·5
31·0
31·5
32·0
32·5
PHASE SHIFTER READING (1 DIVISION = 3·4 DEGREES)
20
22
24
26
28
30
32
34
36

Fig. 10

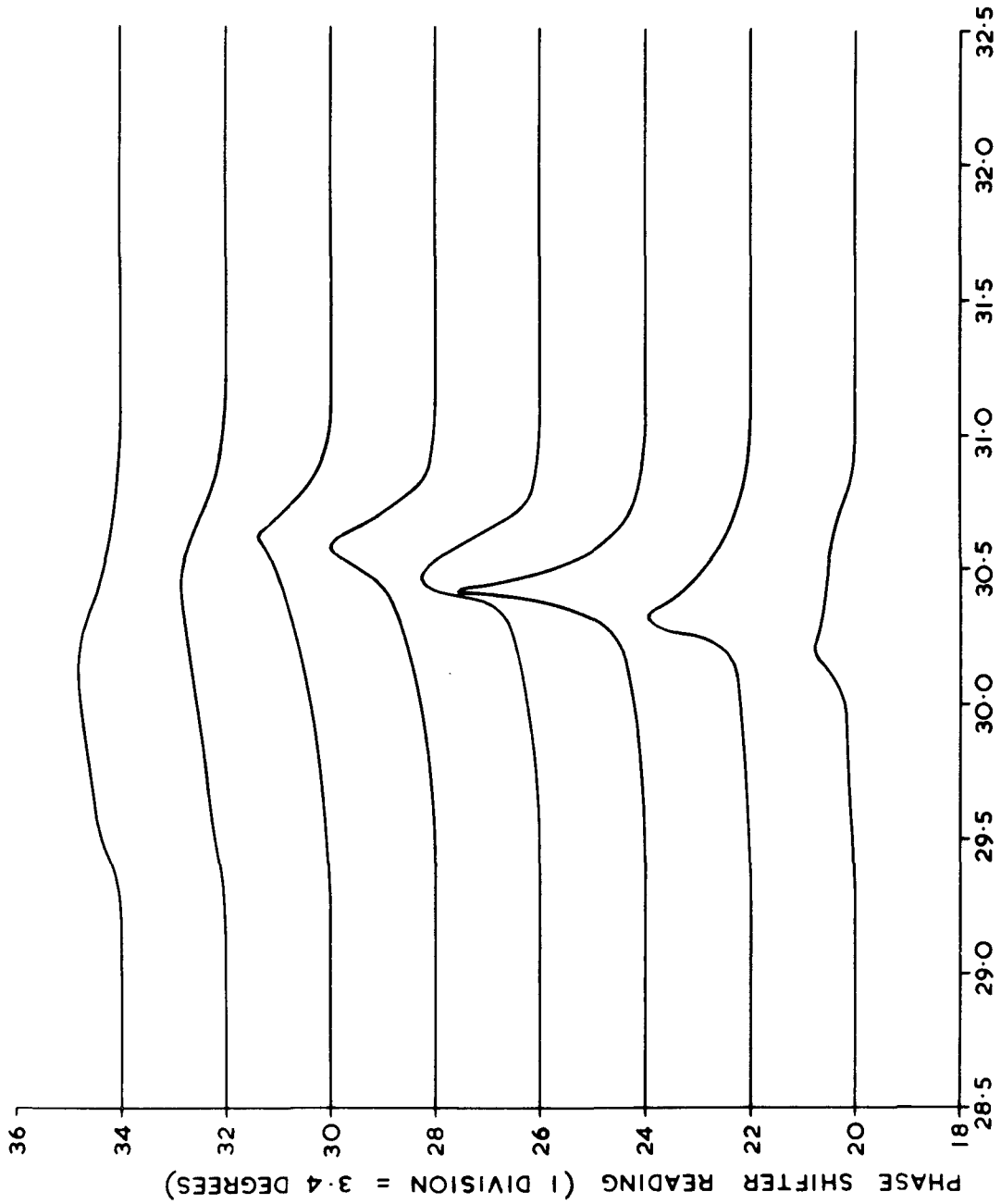
30 MeV ENERGY v INPUT PHASE
TANK 2 R.F. LEVEL = 34·0 (895 KW)
ENERGY IN MeV
28·5
29·0
29·5
30·0
30·5
31·0
31·5
32·0
32·5
PHASE SHIFTER READING (1 DIVISION = 3·4 DEGREES)
18
20
22
24
26
28
30
32
34
36

Fig. 11

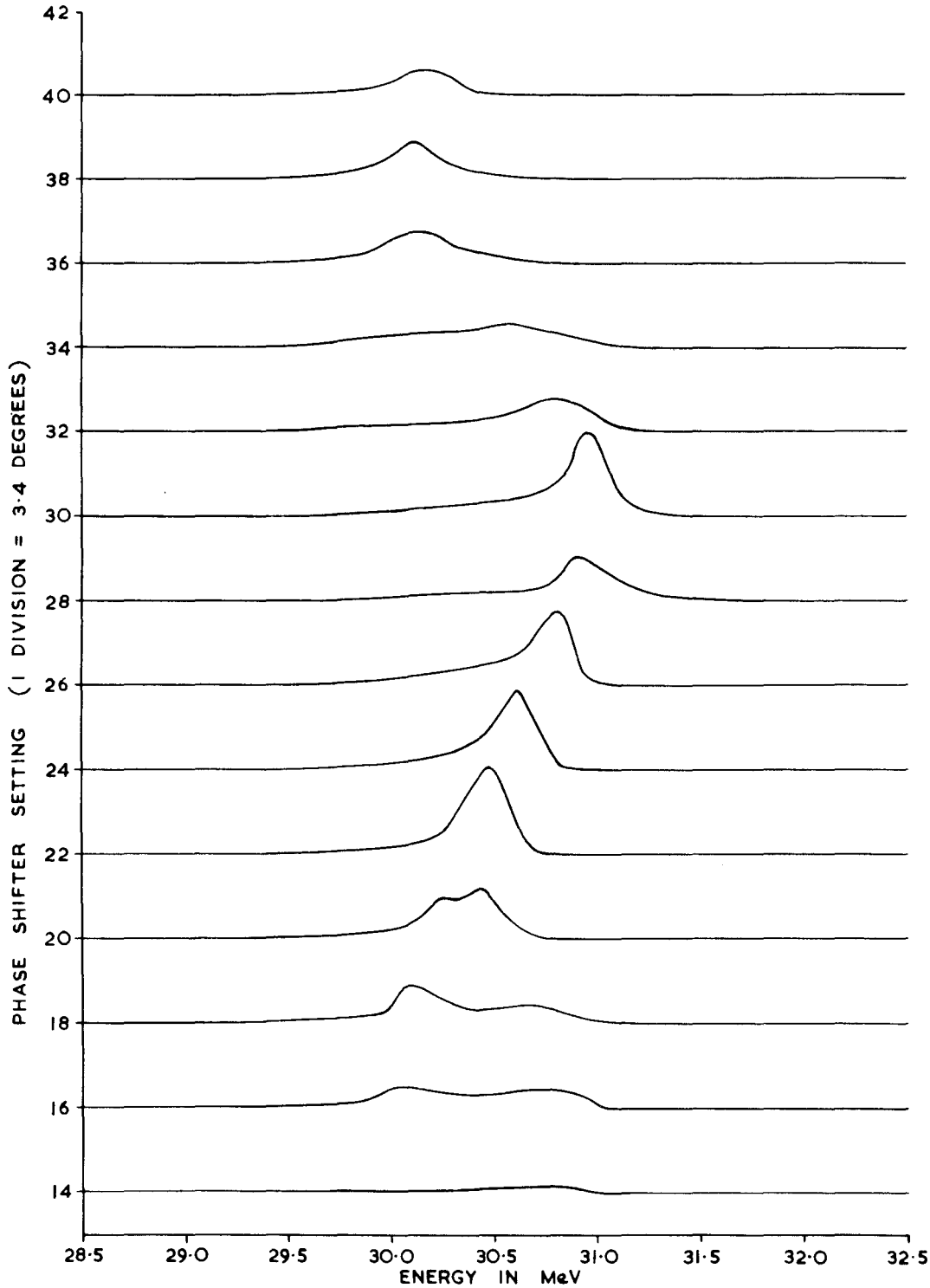

30 MeV ENERGY v INPUT PHASE
TANK 2 R.F. LEVEL = 34·7 (920 KW)

Fig. 12

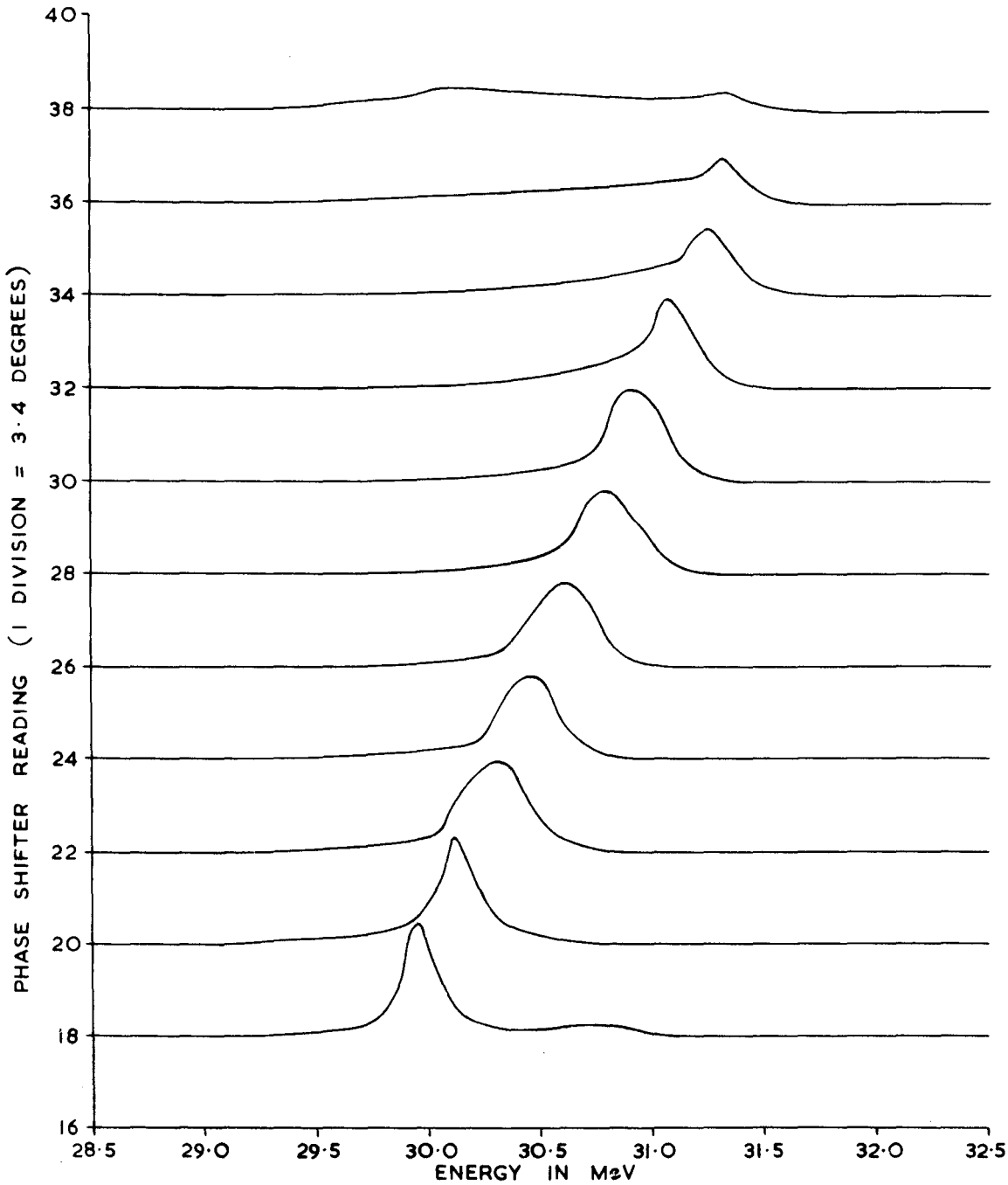

30 MeV ENERGY v INPUT PHASE
TANK 2 R.F. LEVEL = 36 (990 KW)

Fig. 13

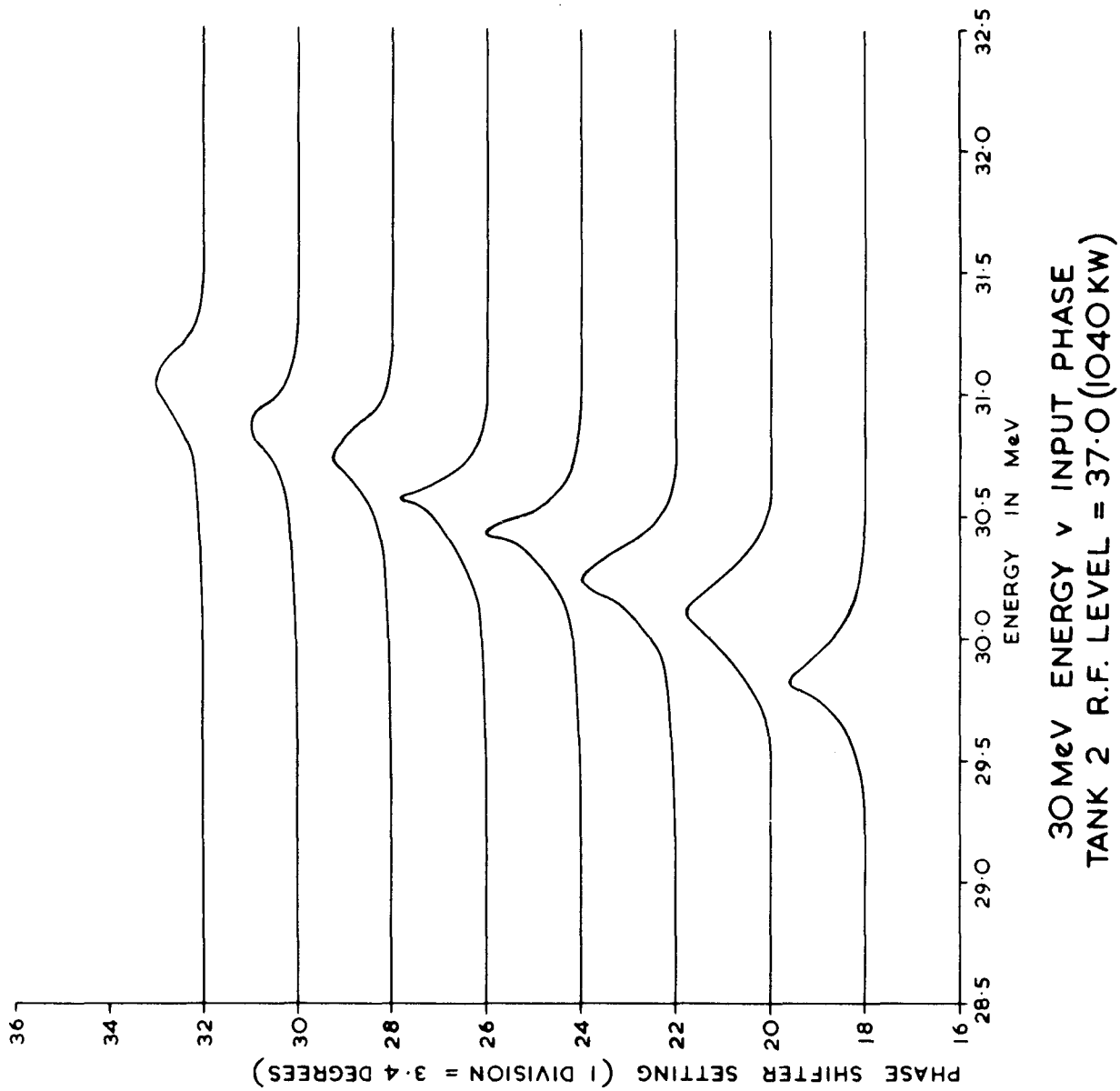
30 MeV ENERGY v INPUT PHASE
TANK 2 R.F. LEVEL = 37·0 (1040 KW)
ENERGY IN MeV
28·5
29·0
29·5
30·0
30·5
31·0
31·5
32·0
32·5
PHASE SHIFTER SETTING (1 DIVISION = 3·4 DEGREES)
16
18
20
22
24
26
28
30
32
34
36

Fig. 14

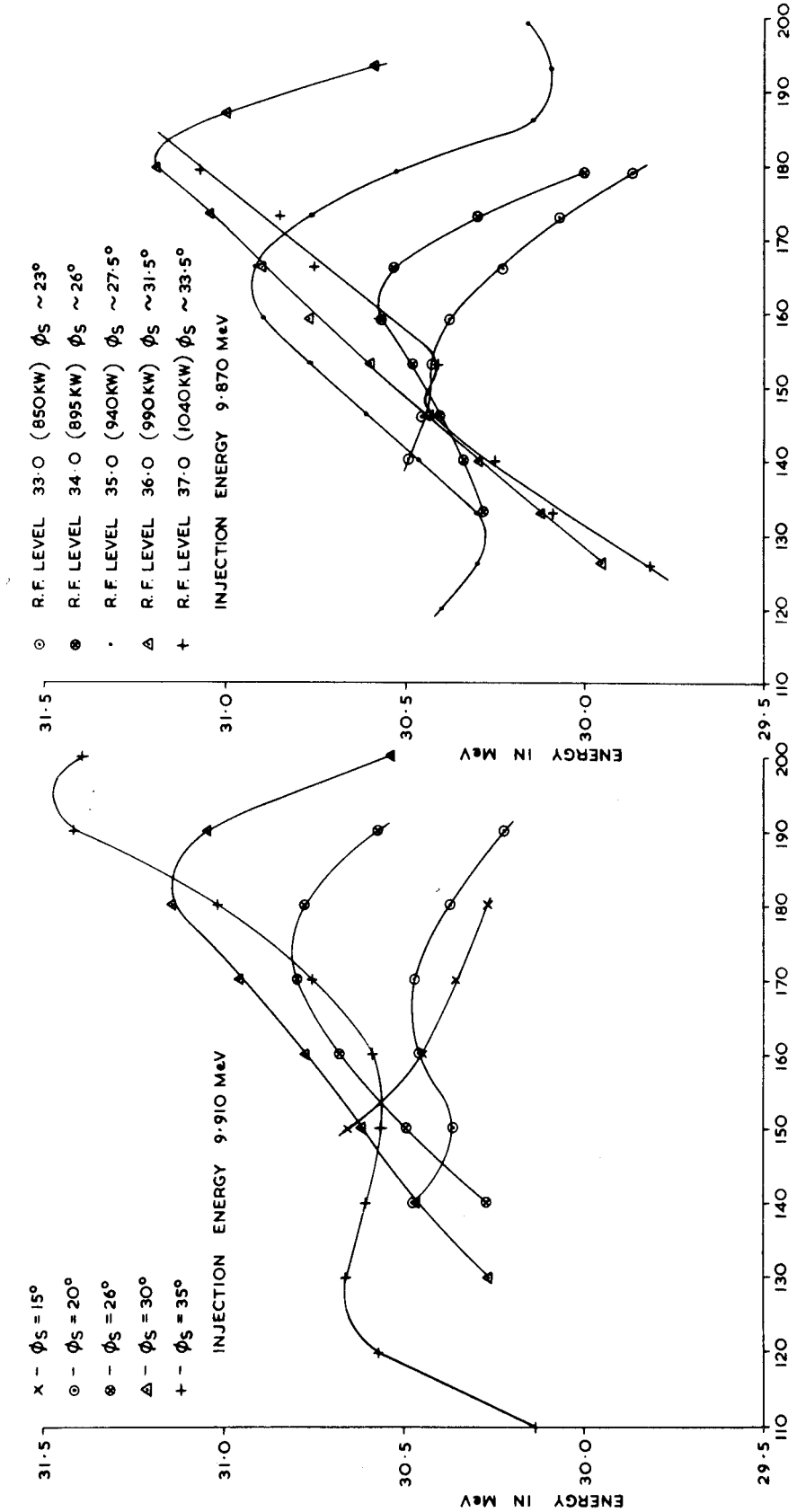
30 MeV BEAM ENERGY v INPUT PHASE FOR VARIOUS R.F. LEVELS
COMPUTED RESULTS
EXPERIMENTAL RESULTS
ENERGY IN MeV
PHASE IN DEGREES
INJECTION ENERGY 9·910 MeV
INJECTION ENERGY 9·870 MeV
x - φS = 15°
⊙ - φS = 20°
⊛ - φS = 26°
Δ - φS = 30°
+ - φS = 35°
⊙ R.F. LEVEL 33·0 (850KW) φS ~ 23°
⊛ R.F. LEVEL 34·0 (895KW) φS ~ 26°
• R.F. LEVEL 35·0 (940KW) φS ~ 27·5°
Δ R.F. LEVEL 36·0 (990KW) φS ~ 31·5°
+ R.F. LEVEL 37·0 (1040KW) φS ~ 33·5°

Fig. 15

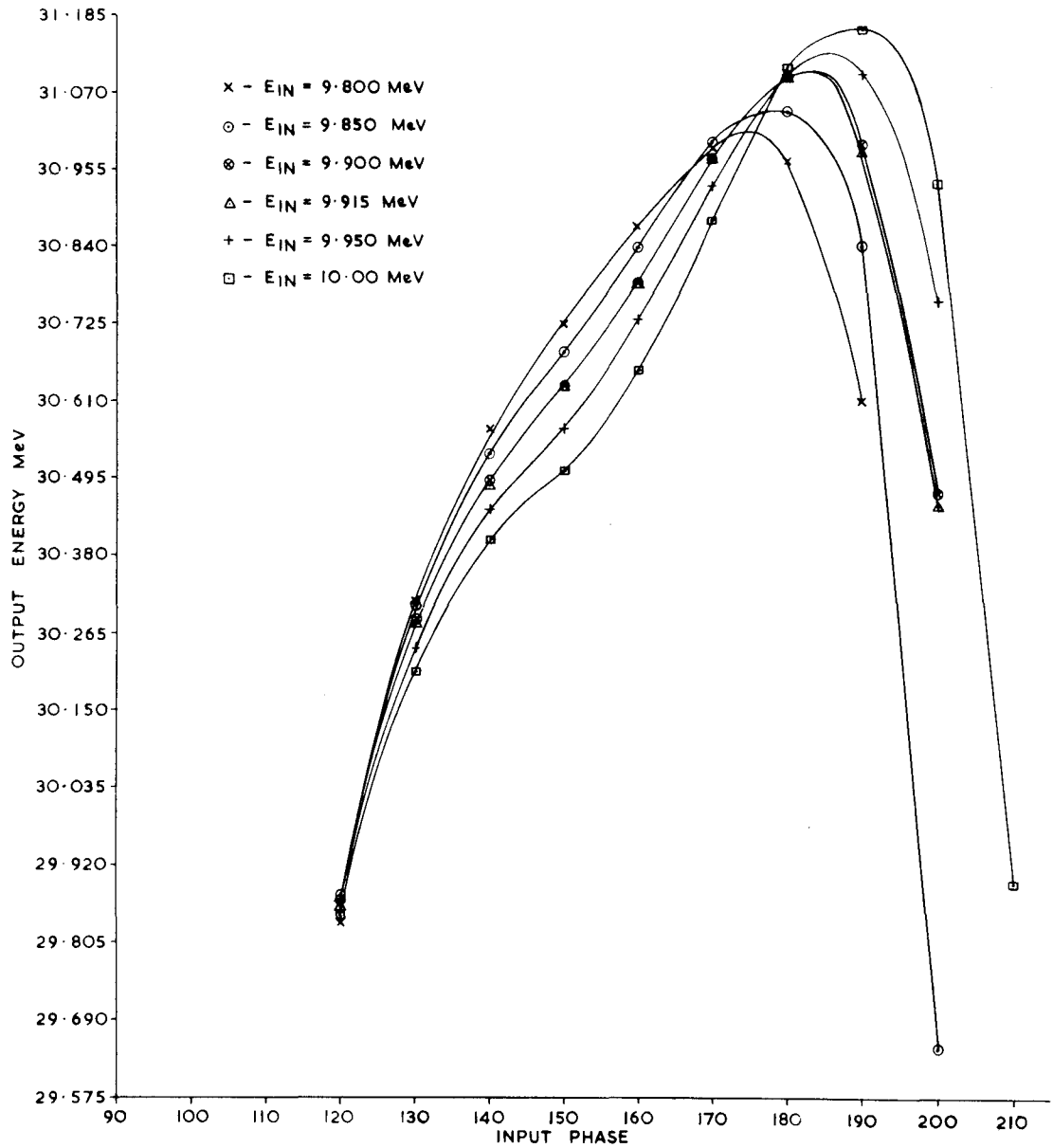

TANK 2
OUTPUT ENERGY v INPUT PHASE
STABLE PHASE 30° & VARIOUS INPUT ENERGIES

Fig. 16

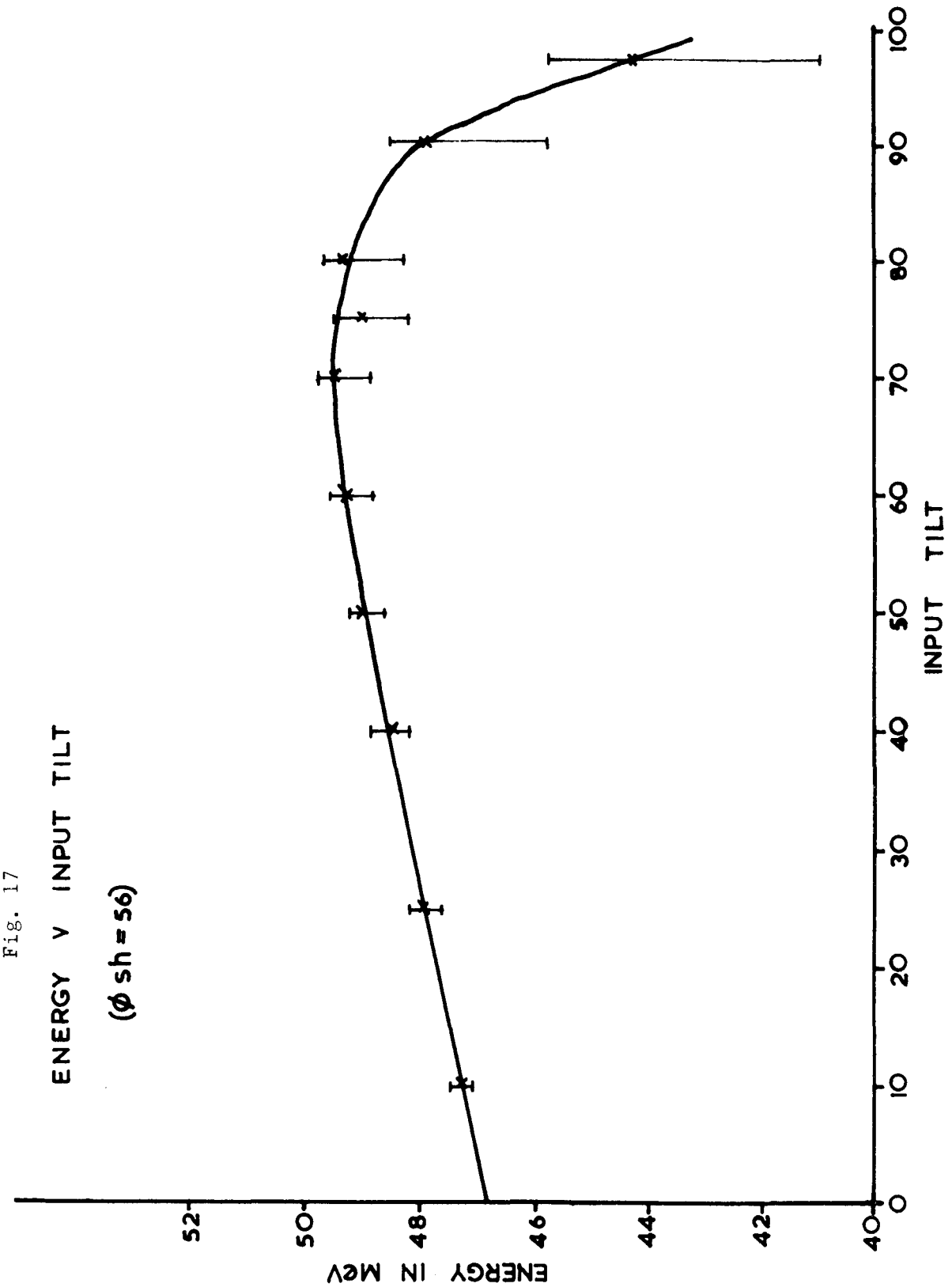
ENERGY V INPUT TILT
(ϕ sh = 56)
ENERGY IN MeV
INPUT TILT
40
42
44
46
48
50
52
0
10
20
30
40
50
60
70
80
90
100

Fig. 17

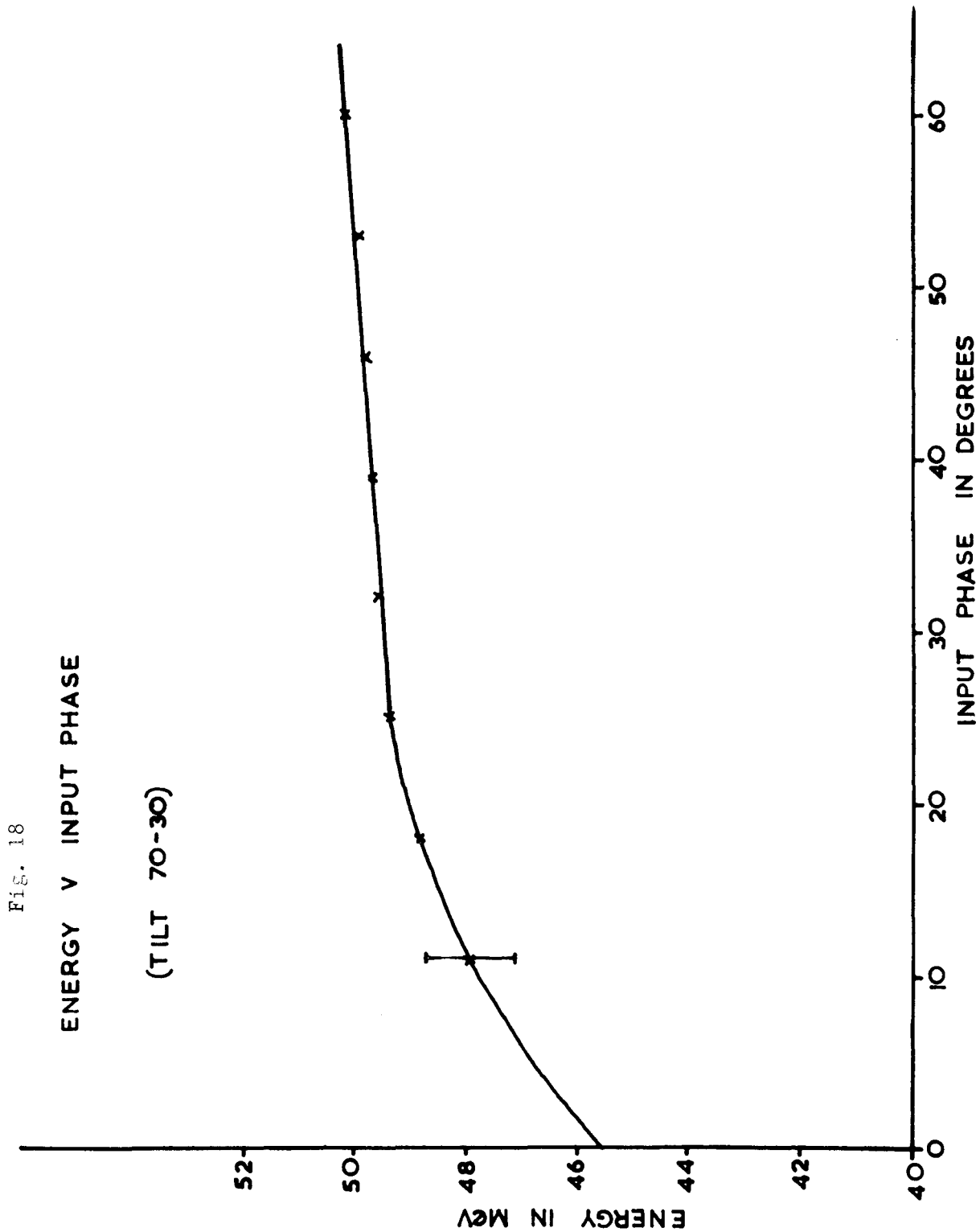
ENERGY V INPUT PHASE
(TILT 70-30)
ENERGY IN MEV
52
50
48
46
44
42
40
0
10
20
30
40
50
60
INPUT PHASE IN DEGREES

Fig. 18